www.czasopisma.pan.pl PAN www.journals.pan.pl
Opto-Electronics Review 27 (2019) 161–173

Contents lists available at ScienceDirect

Opto-Electronics Review

journal homepage: http://www.journals.elsevier.com/opto-electronics review

On the beam radiance of mid-infrared quantum cascade lasers–A review

B. Mroziewicz, E. Pruszyńska-Karbownik*

Institute of Electron Technology, 32/46 Lotnikow Ave., 02-668 Warsaw, Poland

ARTICLE INFO

Article history:
Received 27 December 2018
Received in revised form 29 April 2019
Accepted 2 May 2019
Available online 8 June 2019

Keywords:
Quantum cascade lasers
Laser arrays
Output power
Beam quality factors
Beam
Radiance
Brightness

ABSTRACT

Lasers emitting mid-infrared (MIR) beams have become indispensable for spectroscopy, free space communication or remote security measures. To the one of the most promising families of the lasers suitable for these applications certainly belongs a group of the Quantum Cascade Lasers (QCL). However, among the conditions they must satisfy there is a high enough radiance of the beam they emit. Radiance depends in a complicated way on the laser output power and optical quality of the laser beam. This paper has been devoted to a description and a short analysis of the factors that decide about radiance of so far developed QCLs. Literature concerning both single devices and QCL arrays operating in beam combining systems have been examined and results described. The survey may be useful for estimation of how far the QCLs have come of age.

Contents

* Corresponding author.
E-mail address: ekarb@ite.waw.pl (E. Pruszyńska-Karbownik).

https://doi.org/10.1016/j.opelre.2019.05.001
1230-3402/

1. Introduction

Appearance of quantum cascade lasers (QCLs) in 1994 [1] opened up a long time expected feasibilities for development of semiconductor lasers capable to emit infrared radiation in a wavelength range extending from around 3 μm [2] to terahertz [3,4]. This ability remarkably enhances applications of semiconductor lasers in spectroscopy, free space communications and security, including directed infrared countermeasure systems [5–7]. Spectroscopy takes an additional advantage that in the mid-infrared (MIR) wavelength band the emission linewidth can be as low as 12 kHz [8]. The 3 μm wavelength limit arises due to a small conduction band offset for QCLs made of classic InGaAs/InAlAs structures grown on InP substrates. That can be overcome to some degree by application, for instance, InAs/AlSb compounds grown on InAs or GaSb [2], but this technology is still immature. Extending the QCL's wavelength to terahertz region meets a number of difficulties and requires cooling of the device. Solutions are found either by developing special waveguides [3] or employing intra-cavity terahertz difference-frequency mixing in a dual-wavelength QCLs [4].

Advancements in physics, fabrication technology, properties and applications of the QCLs have been too important and interesting to be left unpublicized. As a result, the number of papers devoted to various aspects concerning these devices is now enormous. In particular, the review papers like those by P. Rauter and F. Capasso [9] or M. Razeghi *et al.* [10] and many more [11–13], both the older and new ones, give a very good survey of the subject.

The purpose of this paper is to draw attention to QCL's beam radiance (termed also brightness) as this feature is in practice the real criterion of the laser performance. That is particularly true for applications that require the presence of high power laser beams at remote locations. Radiance becomes then a laser figure of merit. This topic has been already elucidated by P. Shukla et al. [14] but it was mainly devoted to various types of lasers designed for material processing. In addition, the content of that paper has left some doubts concerning definitions of the laser beam radiance and, thus encouraged us to undertake discussion of the subject.

Our paper concentrates on the analysis of MIR QCL's parameters that decide about their radiance and are deducible from laser properties described in the literature. We have paid special attention to lasers operating within spectral atmospheric windows extending from 4.5 to 5.5 μm and from 8 to 9 μm as they are relatively free of absorption by water (see Fig. 1) and, therefore are most suitable for the systems operating at remote locations.

In addition, the wavelengths corresponding to the first window lend itself to production of high power QCLs. That is because photon energy at (≈275 meV for 4.5 μm) comprises a large fraction of the band offset of conventional lattice matched AlInAs/InGaAs structures (520 meV) and highly strained InP-based material can be used for production of high-performance QCLs emitting at $\lambda < 5.5$ μm using MOCVD or MBE layer growing processes [15–18]. The introduction of the strain leads to higher barriers and, as a consequence, reduces carrier leakage and changes the type of leakage from leakage to continuum to shunt-like leakage within the active region [19]. The QCLs emitting around 4.5 μm wavelengths dominate in research that brings lasers with still scaling up the WPE (Wall-Plug Efficiency) and the output power. This remark by no means disqualifies the 8–9 μm, QCLs also found to be very useful in mentioned above applications. In any case, applications like gas sensing for toxic industrial chemicals and explosives or detection and ranging or free space optical communications the AlInAs/GaInAs structures matched to the InP substrates and grown mainly by MOVPE process dominate in these applications. This remark by no means disqualifies MBE that is still being exploited and delivers excellent QCLs emitting for instance total powers of 4.5 W at room temperature (RT) when pulsed and 2 W CW (continuous wave) with a wall plug efficiency of 16% or 10%, respectively [16], and, thus they are in no way inferior to the best MOVPE-grown QCLs [18]. In any case, the QCLs technology requires careful optimization of the epitaxial process. A non-equilibrium Green's function modelling has proved to be very helpful in examining electronic transport and optical properties of the investigated epitaxial structures [20–22].

Parameters used to describe the performance of semiconductor lasers are, apart from the wavelength, quite often limited to the output power, the regime of the work: pulsed or continuous wave (CW), and the maximal operational temperature. The laser beam itself remains undescribed although as it has been said above, for applications like remote optical sensing it is essential to be able to send the beam of high enough power to a long distance. This deficiency may be partly made up by indicating the so-called beam parameter product (BPP):

$$\mathrm{BPP} = \mathrm{D}_0 \cdot \theta. \tag{1}$$

Here, D_0 is the near-field beam waist width and θ is the beam divergence angle (assuming that it is close to Gaussian). In reality, the beams generated by semiconductor edge emitting lasers both diode and QCL are strongly divergent, radially asymmetric, and by no means can be treated in terms directly related to Gaussian. Despite its deficiency, the BPP factor may sufficiently well characterize the profile of the laser beam that is to be used for applications like welding or cutting. However, much more sophisticated measures have to be considered when the beam is to reach some remote locations. Then, we must know the beam distribution in space and term "radiance" has to be evoked. It is worthwhile to mention that quite often term "brightness" is used instead of radiance despite the fact that we deal with infrared wavelengths. Definition and meaning of radiance have been discussed in Refs. 23 and 24. Here we shall quote only formulas most frequently encountered in the papers dealing with the problems discussed in the present paper.

Thus the radiance can be expressed by:

$$L_e = \frac{CP}{\lambda^2 M_x^2 M_y^2}, \tag{2}$$

where P is the output power, C is some constant dependent on the definition of the beam cross-section dimensions and divergence [25], λ is the wavelength, M^2 is the beam distortion measure in respect to the Gaussian one and, directly from this definition, can be expressed by the formula:

$$M^2 = \frac{\pi}{4\lambda} D_0 \theta, \tag{3}$$

where D_0 is the beam waist width and θ is the divergence angle of the real laser beam [24].

Because there are no unquestioned definitions of D_0 and θ for non-Gaussian beams, it recommended determining the value of M^2 based on the beam matrix **P** containing second-order moments of the Wigner distribution:

$$\mathrm{P} = \begin{matrix} < x^2 > & < x_2^y > & < x\theta_x > & < x\theta_y > \\ < xy > & < y^2 > & < y\theta_x > & < y\theta_y > \\ < x\theta_x > & < y\theta_x > & < \theta_x^2 > & < \theta_x\theta_y > \\ < x\theta_y > & < x\theta_y > & < \theta_x\theta_y > & < \theta_y^2 > \end{matrix}. \tag{5}$$

Then, the beam quality parameter M^2 is expressed by the following formula [26]:

$$M^2 = \frac{4\pi}{\lambda} (\det \mathrm{P})^{\frac{1}{3}}. \tag{4}$$

The beam shape and corresponding M^2 factor have become very important after QCLs came of age and can now operate at room temperature and high output power. The latter and the wide spectral

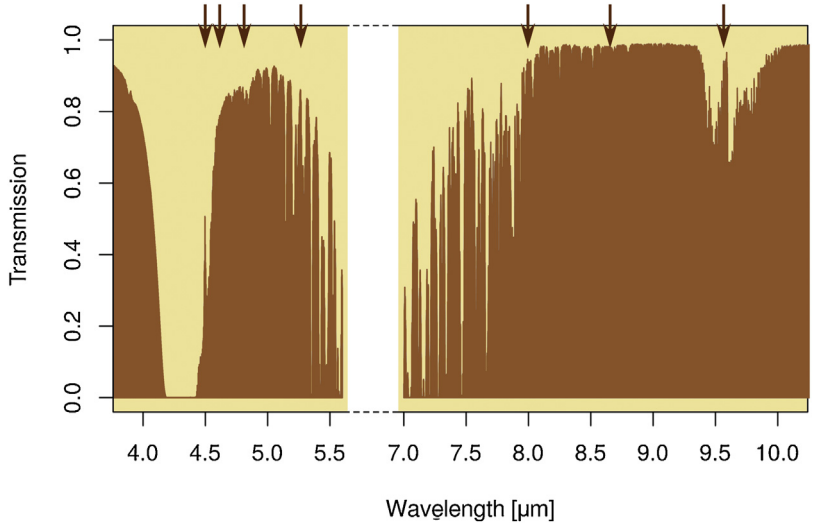

Fig. 1. Diagrams showing transmission spectrum of the atmosphere in the MIR wavelength ranges 4–5.5 μm and 7–10 μm calculated using the ATRAN modelling software [http://www.gemini.edu/sciops/telescopes-and-sites/observing-coditions]. Arrows indicate most common wavelengths of the investigated QCLs.

range in which they operate made them suitable for applications in free space optics if their beams are of high enough radiance.

Unfortunately, the value of the radiance in case of discrete QC lasers is rarely quoted and can be only deduced from the cited output power and M^2 factor, providing that the latter has been measured [27]. Some rough numbers found in the literature are quoted in Table 1.

2. Scaling up radiance of a single QCL

2.1. Output power of a single QCL

High output power is a fundamental parameter in the augmentation process of the QCL's radiance [see expression (2)]. Scaling up the laser output power can be attained by increasing the number of the active region stages, sheet carrier density per stage in the active region or simple enlargement of the laser chip dimensions. All these ways can be exploited to achieve high peak power in pulse operation but most of them are of limited usefulness in the case of CW devices because of their active region self-heating. A high temperature of the active region is detrimental to laser performance as it leads to the higher threshold current, lower slope efficiency and, therefore to lower the wall-plug efficiency (WPE), which in effect diminish maximum optical power of the laser. As these factors are particularly important in case of the QCLs designed to be operated in the CW mode, the active region in such lasers should be designed to suppress the undesirable high-temperature effects and to provide effective heat dissipation from that region. It should be, however, remembered that enlargement of the waveguides width results in lower beam quality due to excitation of a multimode operation. On the other hand, the increase in the laser cavity length does not cause any increase in the active region temperature and does not affect the beam quality. Thus, the advantage of this approach is that high power can be obtained from narrow devices which are less subject to self-heating and are therefore less sensitive to limitations such as the thermal conductivity of the sub-mount. In the range for which there is the gain not saturated, the WPE in pulsed operation depends theoretically on cavity length only through mirror losses, so it can be maximized for a given cavity length by deposition of a facet coating that will produce the same mirror losses as those for the optimal length. In result, the output power of QCLs can be increased while maintaining high WPE by using long cavities and optimized AR coating [28]. It is to be noted, however, that the CW WPE strongly depends on the laser slope efficiency the latter being the result of *inter alia* injection efficiency inherent to the mechanism of QC laser operation and losses in the laser structure. In particular, the slope efficiency is decreased by carrier leakage through the inactive stages or increasing of the electron backfilling the lower laser levels. This efficiency clearly depends on thermal losses in the laser chip and its value is also related to the laser lateral beam mode content. The last word has not yet been said, however, just recently [29] it was found that old-fashioned GaAs QCLs can be still improved by deepening all the GaAs wells in the laser structure, both in the active region and injectors. The effect was attained by increasing amount of indium in these wells and resulted in devices that could operate up to 323 K.

For high power devices, the situation may be complicated by non-uniform gain saturation due to variations in longitudinal intensity profile along the waveguide. This may have a detrimental effect on the WPE in case of very long devices (*i.e.* longer than centimetre ones) and such optimization does not lead to high power lasers. Although the losses can be reduced to a certain extent by optimizing the laser facet coatings, this way turned out not very effective for high power devices [30]. In any case, mirror losses must be optimized with regard to WPE by deposition of a facet coating properly adjusted to the cavity length.

It is obvious that heat dissipation from the laser active region depends strongly on the laser geometry. With reference to QCLs, their structures can be grouped as shown in Fig. 2.

Most QCL configurations described in the literature have been designed in form of the index-guided narrow waveguides (i.e. of the width not exceeding 10 μm) to avoid high order modes and improve heat dissipation through side waveguide walls. The optical waveguide, in general, should provide low optical losses and a large overlap factor of the optical mode with the gain medium. An interesting configuration of a high power QCL has been described in Ref. 31 and shown in Fig. 2b). Its design is an alternative to the typical design called double channel [Fig. 2a)]. A narrow width low-ridge configuration is exploited for achieving high peak pulsed power. The basic mechanisms that play here a role are changes in the lateral current spreading in the layers above the active region. The narrow waveguide can take in addition an advantage of the current spreading that leads to a lower threshold current density due to the mechanism of their operation. But the narrow waveguide QCLs, in general, suffer poor heat sinking because of the low heat spreading area. A solution is the buried double channel ridge heterostructure

Table 1
The QCL's radiance values selected from the literature to illustrate chronologically the achievable magnitude of this parameter.

Year	Ref. No	Peak power [W]	M^2	λ [μm]	L_e [Mwcm^{-2} cm^{-1}]	Operation	Design
2010	66	9̃	3.5	4.36	3.86	Pulse	Broad area PC DFB
2010	80	0̃.3	< 1.4	4.48	1.73	CW	CBC in the Michelson cavity
2010	91	30	<2	4.6	35.4	Pulse	WBC of QCL array beams in the external cavity system
2011	85	0.5	(x) 1.2 (y) 1.6	4.65	1.38	CW	Beam combining with Dammann grating
2011	38	2.5 (*1.36*)	(x) 1.06(y) 1.03	4.65	10.6	Pulse (*CW*)	Buried heterostructure
2013	65	4	1.6-1.8	8.1	3.35 – 4.05	Pulse	MOPA tapered
2013	64	2.5–3.8	2.08 2.25	9.5	1.40 1.87	Pulse	MOPA tapered (FWHM 1°) (FWHM 2°)
2013	61	2	1.3-1.6	9.2-9.7	0.63 – 1.6	Pulse	MOPA tapered
2014	53	1.25 1.2	1.24-1.98 3.85	8.7	0.07 – 0.72 0.34	Pulse	Tilted front facet
2015	55	203	5	4.8	156	Pulse	Angled cavity
2016	41	23.5	(x) 6 (y) 1.27	4.55	14.89	Pulse	Gain-guided

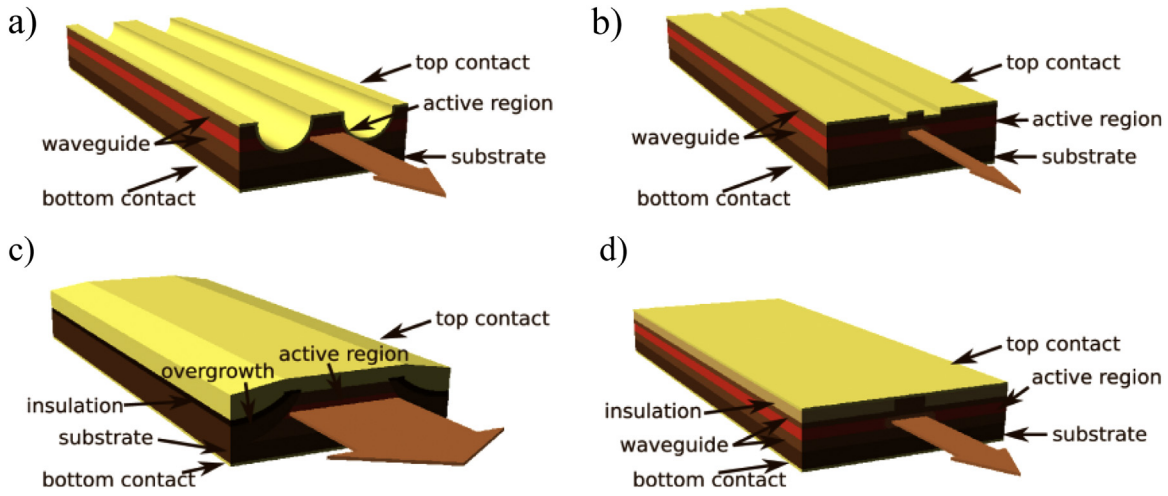

Fig. 2. Schematic drawings of the currently existing QCL's designs: a) double channel high mesa, b) narrow low ridge, c) buried ridge waveguide, d) high-power gain-guided.

(BH) [see Fig. 2c)] having a narrow width of the ridge [32]. That approach turned out to be the most effective way to achieve the required parameters and in addition to maximize the heat dissipation from the waveguide core [33–35]. These features combined with improvements in active region design dramatically increased the WPE in recent years. The active-region designs that reduce the carrier leakage evolved from the deep-well design [36] to so-called shallow wells [33] and so-called step-taper active region [18,19]. While in 2009, the QCLs emitting in the 4.6 μm window delivered 3 W CW with WPE of 12.7% at 293 K [34], two years later in 2011, the attained CW WPE at RT for InP based QCLs, emitting around 4.9 μm, was of 21% and raised to 27% in pulse operation [37]. The maximum CW RT power output of these lasers reached 5.1 W. However, due to such enlargement of the waveguides, the laser operation must be multimode and, as mentioned above, results in poor beam quality. Xie *et al.* [38] showed that deterioration of the beam quality of QCL emitting about 4.6 μm starts for the waveguide width of 7 μm. Record high pulse power of 120 W was achieved by enlarging the ridge width up to 400 μm although at the same time the WPE showed some decrease [39]. Whereas, the record of CW single-mode power from broad area (BA) QCL is 1.36 W [38]. A more detailed analysis of the BA structures has shown that a wide active region does not prohibit the RT CW QCL's operation [40]. Lasers with the active region 30 μm wide, and consisting of only 10 cascades, emitted 0.6 W CW at temperatures close to RT. In order to achieve this, it was necessary to provide conditions for effective heat sinking from the top contact and to limit the thickness of the active region by restricting the number of cascades. The laser should be mounted epi-down applying well known already methods and materials. Temperature distribution in the BA QCLs described in Ref. 40 leads to the conclusion that temperature rise in the active region scales linearly with the heat density, but is squared with the active region thickness. Therefore, it is adventurous to decrease cascade number even if that will increase heat density due to the rise of the threshold current density. Thus, the increase of the laser ridge width can be considered as a promising route to scaling the laser output power. Unfortunately, at this approach, the beam profile degrades quickly as higher order lateral cavity modes are excited. In result, the BA QCLs tend to show multiple peaks in the far-field profile due to exciting higher order lateral modes and a "rabbit ear" shape in the far field is the typical beam pattern for BA QCLs. It is so if no special precautions are taken and the TM polarization facet reflectivity increases with mode index. The broad area QCLs lase in that case on high order modes with a far-field profile consisting of 2 lobes propagating at large angles from the optical axis. Nevertheless, the BA geometry is the most straightforward approach for power scaling of the QCLs. Due to the increase in the size of the resonator the output power can be hundreds of times higher than in the case of a narrow ridge device. As mentioned above up to 120 W peaks power has been demonstrated in a BA QCL. However, both high output power and good spatial beam quality of BA QCLs can be achieved only by suppression of higher order lateral modes. Despite all the drawbacks, the BA QCLs are very interesting because, unlike diode lasers, in general QCLs have negligible linewidth enhancement factor [31] and therefore should not suffer from filamentation and consequently

could operate stably in a single transverse mode at currents well above threshold.

The lasers described above belong to the group termed "index guided" adequately to the way the mode structure is formed. The other type of that process may be "gain guiding". Gain-guided diode lasers have been known for decades. They generate high power beams but with rather poor quality. In that aspect, the QCL's designs demanded a different approach from the described above. Therefore, on a special notice deserves described in Ref. 41 idea leading to high power gain guided QCLs based on the structure that assures operating at fundamental optical mode. In that structure [see Fig. 2d)], distribution of the current in the active region became strongly non-uniform and gain profile corresponding to the horizontal current density spreading led to gain guiding and efficient optical mode selection. Described lasers emitted 23.5 W peak power at RT and 1% duty cycle. Due to their efficient optical guiding, they emitted a single lobe beam with a ratio of 1:7 between the horizontal and vertical axis. The estimated value of $M_x{}^2$ was around 6. Unfortunately, the output beam characteristics depended strongly on the current.

In conclusion, it is quite difficult to develop QCLs emitting a high power beam and to avoid at the same time an increase of the M^2. Thus, achieving solely emission of high output power is not enough to attain a laser beam of high radiance.

Regardless of the laser structure, heat generated in the device must be effectively conducted away. This necessity has impelled to extensive research on heat spreading in semiconductor lasers [42–44]. Particular effort has been devoted to soldering process of the laser chips to heat spreaders. This task has been challenging as both the heat conductivity of the soldered materials and the strain between them had to be taken into account. Significant improvement was achieved when so-called epi-down soldering technique based on using a hard solder (AuSn) has been mastered [42]. Any research on these problems obviously demanded development of measurement techniques capable to evaluate temperature profiles within the laser active region. In that aspect, thermo-reflectance spectroscopy turned out to be very helpful and has been studied in details [45,46].

The obvious solution leading to scaling the laser output power is to operate it in a pulse regime and that is a common practice. It is important that in a pulse mode operation the laser output power increases linearly with the width of the device. Still, it should be noticed that an intra-pulse modal instability and beam steering in a pulse operated QCLs may take place due to lateral hole burning [47].

Recapitulating the remarks above one should be aware that in addition to edge emitting lasers there exists a plethora of another laser configuration as described below.

2.1.1. Linewidth and tuning of QCLs

The QCLs as a source of penetrating signals provide very powerful technical solutions applicable to spectroscopy used at remote allocations. They can be designed to operate in a single mode with a very narrow linewidth and sufficiently high pulsed or CW power that satisfy spectroscopy requirements. For instance, the power of 2.4 W CW has been attained in a single lobe with a side mode suppression ratio (SMSR) around 30 dB in the current range of 1–1.7 A [48]. As mentioned above, the linewidth as low as of 12 kHz was estimated for a stabilized QCL [8]. The required single mode operation of the laser is usually achieved by implementing the distributed feedback (DFB) configuration. For a CW operating DFB QCL, a free-running frequency stability of 150 kHz over a 15 ms time interval has been observed [49].

Tuning of the laser wavelength is absolutely necessary for spectroscopy applications. The simple DFB QCLs can be tuned either by changing the supply current or temperature. The best results

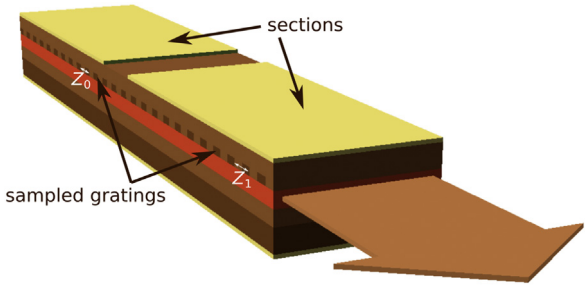

Fig. 3. Schematic of a multi-section sampled grating DFB QCL.

obtained for the current tuning of 4–5 μm QCLs were of the order of 5 cm^{-1} [48]. Temperature tuning is slightly more effective and was executed over a range of 6 cm^{-1} for DFB QCLs operating at $\tilde{9}$ μm. This figure could be multiplied by combining lasers to form an array with individually supplied lasers [50]. A much better solution relies on a multi-section sampled grating DFB (SG DFB) technology [51]. An example of such solution is displayed in Fig. 3. It consists of two sections each containing gratings with sampling periods Z_1 and Z_0, respectively. Both sections utilized a 30-period grating which was sampled 3 times. The sampling periods were appropriately adjusted for different sections to obtain uniform injection tuning effects. The obtained tuning range was up to 50 cm^{-1}.

It is true that internal tuning range limitations connected with DFB QCL structures can be overcome by applying configurations based on external cavity feedback. The 303 cm^{-1} tuning range was obtained for a DFB QCL operating at the central wavelength of 8 μm with a maximum optical power of 200 mW [52]. However, these systems require external optical components and their tuning is of a mechanical nature. As such, it is slow and dependent on the mechanical precision.

2.2. Scaling up the radiance by minimizing the value of M^2 factor

As it has been shown above, the most straightforward approach leading to scaling up the QCL output power is increasing the geometric dimensions of the laser. However, simply widening the laser cavity leads to poor beam quality and multimode spectrum arising from high-order transverse modes.

If a high power QCL is engineered by the increase of the device area, its beam profile usually degrades. It is because higher-order lateral cavity modes are excited and this results in the increase of M^2. An exception has been described above with reference to gain guided QCLs, but the obtained results demand further improvements. In any case, high output power is not enough to obtain the laser beam of high radiance. Making simply the resonator wider but without changing its shape would induce a degradation of the beam quality. In fact, a mentioned above rabbit-ear-shaped far field is the typical beam pattern for BA QCLs.

An interesting solution to this problem has been found by tilting the laser front mirror (facet) with respect to the optical axis of the cavity [53]. The non-perpendicular cavity has been realized by a specific etching of the front mirror that makes them nonparallel. Such mirrors induce asymmetric light intensity distribution along the laser cavity and hence most of the light is being emitted through only one facet. In the cited work, emission through the tilted front facet has shown a lower beam divergence, suppression of higher order lateral modes of BA QCLs, as well as the increase of slope efficiency and of the maximum peak power. The optimal tilting angle was around 17° and the method was effective to the waveguides of about 60 μm wide. The peak output power of 1.3 W in a single lateral mode has been obtained and the lasers showed a nearly-diffraction-limited beam with an FWHM of 8.3°.

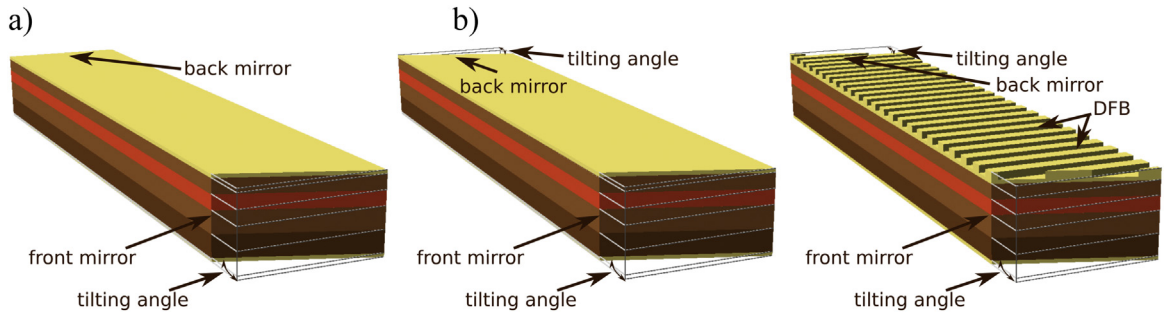

Fig. 4. Principle of a" tilted mirror" QCL (a) and two exemplary types of" angled" QCLs (b) (based on ideas presented in Refs. [53–55]53–55).

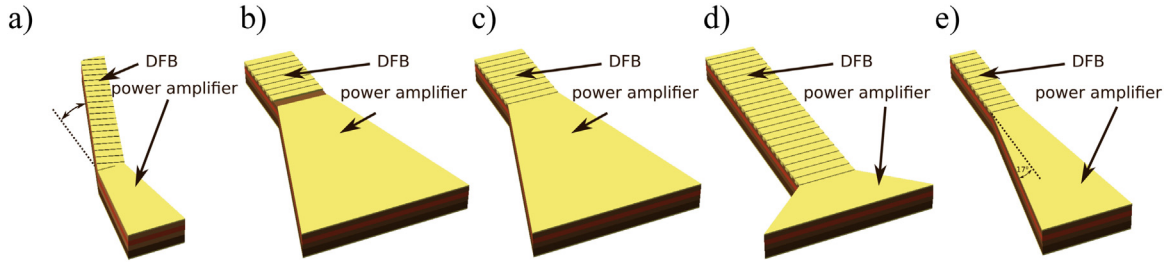

Fig. 5. MOPA and tapered laser designs devised to emit high radiance beams.

The calculated M^2 value depended on the current and was around of 1.24–1.98 resulting in the radiance of 0.07–0.72 MW cm^{-2} sr^{-1}, respectively.

A similar approach but with two laser facets tilted with respect to optical axis was proposed for DFB QCLs and termed "angled cavity" [54,55]. The concept of both solutions has been displayed in Fig. 4.

As a result it has been proved that angled waveguides, as well as DFB and photonic crystal DFB QCL angled cavity with parallel facets, bring power scaling with good beam quality and so provide a high radiance. However, it should be noted that these lasers work only in the pulse regime, which still does not diminish their usability for some applications, such as molecular spectroscopy. As the angle increases all modes experience increased losses, but the higher order lateral mode losses intrinsically increase faster than the fundamental mode. This is due to the nonlinear relation between the penetration depth and the incidence angle and provides lateral mode discrimination. For any wavelength, exists a critical angle for suppressing the higher order modes. This angle is dependent on the side wall shape, its roughness, and materials. The study on the tilt angle was carried out on QCLs with double channel waveguide emitting around 5 μm [55]. The tilt angle was on the order of 12° and a peak power of 203 W was obtained at the driving current of 136 A for a duty cycle of 0.02%. At a driving current of 120 A, the M^2 = 5 was obtained with an FWHM of 3°. The output power at this current was 180 W which translates to a record high radiance L_e of 156 MW cm^{-2} sr^{-1}. This ultrahigh radiance value for a QCL may be considered as a proof that the single lobed far field is due to the angled cavity.

Combining the sampled grating solution with the surface emitting concept one can obtain an interesting result in form of a narrow beam as described in Ref. 56. The quoted laser has been termed "grating-coupled-surface emitting QCL" (GCSE). A 2nd order DFB/DBR Au-semiconductor grating was used for feedback and outcoupling. The DFB grating was terminated on each end by second-order DBR gratings. Grating periods have been adjusted to generate a single mode beam which was perpendicular to the active region plane and that has led to surface emission. Laser operation has been made possible by inherent suppression of the antisymmetric modes and therefore depended on phenomenon connected with the resonant coupling of the guided optical mode to the antisymmetric surface plasmon mode of a metal–semiconductor grating. The laser operated in a symmetric grating mode at 4.75 μm wavelength and emitted around 0.4 W in a single lobe of 0.048 °FWHM. The emission linewidth was of 0.43 nm. It was found that such laser configuration does not affect the laser output power while collimates the beam. Further improvements of this device concept are expected.

2.3. MOPA QCLs

Laser configuration termed MOPA (master oscillator power amplifier) is one of the most promising approaches to scaling up semiconductor laser beam radiance in the pulse regime. They owe this to combining a seed *i.e.* the laser that generates high optical quality signals with an amplifier that if properly designed, amplifies the output power without significant distortion of the output beam. The idea of MOPA structures originated at times when choice of seeds and power amplifiers was at the beginning restricted to diode laser structures. It became particularly interesting after power amplifier section took the form of so-called "tapered waveguides".

The first proofs-of-concept of the QCL MOPAs were demonstrated by Trocolli *et al.* [57] and they soon found followers. The investigated devices have been of different geometry depending on the expected laser properties. However, all of them consisted of two parts: a seed operating as a DFB laser and a section of a power amplifier (PA). Their layouts have been sketched in Fig. 5. The PA section has been at the beginning rectangular, afterwards "tapered" to exploit many advantages of this geometry among them the possibility of a single lateral mode operation. In high power lasers with the broader active area the PA section mitigates the effect of gain saturation on reducing the single-pass gain. To prevent lasing in this section the front facet can be AR coated or cleaved at a small angle relative to the normal with regard to the propagation direction [see Fig. 5a)]. Depending on the version, the seed and PA can be electrically connected or supplied separately [58] (types *b* and *c* in Fig. 5). A disadvantage of electrical isolation between the MOPA sections is

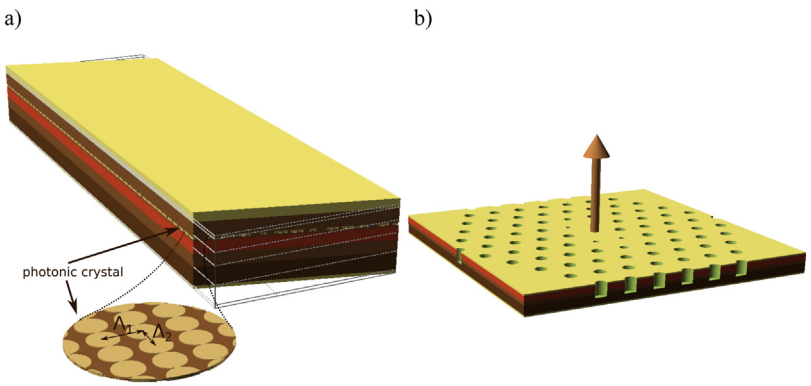

Fig. 6. Configurations of (a) a photonic crystal DFB QCL (based on idea presented in [66]) and (b) photonic crystal surface emitting QCL (based on idea presented in [69]).

the necessity of double synchronized supplying. In the electrically connected version, the whole MOPA configuration with tapered PA can be considered as a "tapered laser". Concluding, it is obvious that configuration of the tapered MOPA QCLs offers many solutions to satisfy properties demanded from these devices *i.e.* high output power and/or single transverse mode operation that leads to high radiance. Their geometry allows in general for suppression of higher-order lateral modes because of taper acute angle while the increase in the volume of the gain material over that of conventionally designed ridge devices results in a significant increase of the available peak power. Therefore, the sections of the tapered MOPA lasers sketched in Fig. 5 may differ not only in width but also in length (types *c* and *d*). In type *e* the main purpose of the taper was to increase the device area in order to increase its peak power in low-duty-cycle pulse operation while maintaining good beam quality. In such devices, the length of the tapered section was typically more than half of the entire device [59]. The purpose of shaping the PA in form of a taper may also be reducing optical intensity at the output facet to increase optical damage threshold while keeping self-heating to a minimum for high-performance CW operation. Therefore, the taper width and length, in that case, is kept to a minimum leading to coversion from MOPA to flared waveguide [60]. These lasers showed WPE of 16.3% and optical power over 4.5 W CW in 283 K. They had highly strained active region composition and operated at 4.7 μm wavelength. Single-longitudinal and single-spatial mode tapered pulsed QCLs have been described in Ref. 61. An evident advantage of a tapered MOPA configuration over typical Fabry-Perot (F-P) cavity has been shown in Ref. 62. The output power of 1.5 W at RT (λ =7.26 μm) was obtained for tapered MOPA QCLs while only 0.9 W was available from the F-P QCLs made from the same MOVPE on InP grown active region material. The MOPA tapered lasers displayed single longitudinal and transverse mode emission which resulted in the beam FWHM of 10° in the chip plane. This figure was 3 times higher for the F-P structures. Non-linear flaring of waveguides has also been tested recently and although the linearly tapered waveguides produce the greatest output power, convex waveguides lead to better beam quality and consequently greater radiance [63]. In another type of lasers the light emitted by the seed travels only once before leaving the device, thus the taper section was used as a monolithically integrated single pass external optical amplifier for obtaining high output power [64]. The length of the tapered section was chosen so that the taper angle was of 0.7° and the mode expanded adiabatically in this section. Thus, the taper was used as a monolithically integrated single pass external amplifier, *i.e.* a device through which the light emitted by DFB oscillator travels only once. Although the slope efficiency decreased with increasing taper angle, paradoxically, the threshold current density was also lower for the tapered devices than for the F-P device made from the same material. This has been explained by the fact that threshold current density is also lower for the tapered devices than for F-P lasers. The 1.0° devices delivered up to 2.5 W of optical peak in the beam with M^2 = 2.0°. The devices emitted 3.8 W with M^2 = 2.25 and had the radiance of 1.87 MW cm^{-2} sr^{-1} [64].

In attempt to attain a QCL that would emit the beam of possibly low divergence a MOPA with plasmonic collimator has been developed [65]. The collimator was produced on an InP laser substrate in the plane of laser facet. It consisted of a second order grating with 7.5 μm period. The obtained M^2 value was of 1.6 at $I = 3.5 \cdot I_{th}$ and therefore the maximal radiance of 4.05 MW cm^{-2} sr^{-1} was reached (see Table 1).

2.4. Photonic crystal (PC) DFB QCLs

Although the gain guided QCLs based on a wide active region and a narrow current injector on the top, attained peak power emission of 23.5 W at RT (see Ref. 41), the problems of the beam quality and scaling up of the M^2 factor have not been solved. In search for new QCLs configurations that would lead to improvement of both these parameters a two dimensional photonic crystal structure distributed along the cavity has been proposed and investigated [66]. Its configuration is shown in Fig. 6a). Other use of photonic crystals, as shown in Fig. 6b), results in surface emission and the lasers are termed surface emitting photonic crystal QCLs [69].

The photonic crystal distributed feedback (PC DFB) structure described in Ref. 66 had a form of the rectangular lattice with first and second order Bragg gratings in the transverse and longitudinal directions. The aspect ratio of the resulting rectangular structure was $\square_1/\square_2$ = 2. The cavity facets were tilted at the angle of 14^0 with respect to the transverse axis of the lattice. At a cavity width of 100 μm high-power nearly-diffraction-limited operation up to 6 W was obtained from the PC DFB QCL. The radiance of a PC DFB laser increases with increasing cavity width and optimization of this parameter is a major concern in the design of high-performance BA lasers [66]. A 400 μm wide PC DFB QCL emitting at λ =4.36 μm with a total peak power of 34 W at RT based on an optimization of the coupling coefficients at the given cavity width and length has been realized, its slope efficiency was around 560 mW/A [66]. The M^2 parameter had value of 2.5 at 1.1 I_{th} and stayed below 3.4 up to 1.51 I_{th}. The radiance of these lasers was increasing with enlargement of the cavity width. The power output was strongly related to the beam quality and single spectral mode operation through the selection of transverse and longitudinal coupling coefficients at a given cavity width and length could be achieved. It is worthwhile noting that QCLs should not suffer from filamentation and thus could operate stably in a single transverse mode at currents well above threshold. But because of a TM polarization, facet reflectivity increases with mode index and broad area QCLs are lasing on

a higher-order mode and the far-field profile consists of 2 lobes propagating at large angles from the optical axis. The beam divergence along the fast axis is usually controlled by lenses. However similar results can also be obtained by shaping the output beam by plasmonic collimators coupled to the front face of the laser [65].

3. QCL arrays

While individual QCLs are slowly reaching limits of their output power, even when operated in pulse regime, there are new horizons opened up by assembling them into arrays [61]. So far, the most spectacular solutions are based on individually addressed DFB QCL arrays with a frequency span of 85 cm^{-1} [9]. This classic solution was based on an array of 32 DFB QCLs with closely spaced emission wavelengths. This spacing was sufficiently small to allow for attaining any desired wavelength within the laser gain spectrum. In addition, by heating an individual DFB laser, its wavelength could be well adjusted. The advantage of the QCL arrays over the external cavity QCLs stems from the monolithic structure of QCL arrays and their fully electronic wavelength tuning that allows for avoiding any moving gratings and thus realizes higher speed acquisition and wavelength stability.

The array sub-beams, however, could not be collimated properly with a lens because each of the lasers in the array emits at a different angle with respect to the optical axis of the system. In result, the collimated beam would consist of many wavelengths emitted by individual lasers in the array and all that would cause detrimental interference. In addition, each beam in the QCL array is radially asymmetric. Other problems that appear are induced by thermal management of the heat produced in the complicated arrays configurations. Discussion on that subject can be found in the cited above [44].

3.1. Internal phase-coupling of the laser array modes

Intuitively it could be imagined that the most elegant way leading to synchronization of the beams generated by lying side by side lasers in an array could be realized by globally coupling all waveguides. This phenomenon has been a subject of many years research carried out on diode laser bars at least from the year 1988 (see Botez *et al.* [67]) and devoted mostly to anti-guided diode laser arrays [68]. They had been afterwards switched to QCLs and the results described in numerous papers among them devoted to Surface-Emitting Photonic Crystal Lasers [69] and other designs [70–72]. The new achievements looked promising but it turned out that even in the case of wavelengths close to near-infrared, this method is troublesome as the needed fabrication tolerance (which is proportional to the wavelength) is in the order of 0.1 μm. That changed dramatically when QCLs operating in the MIR band appeared. The experiment with QC laser arrays emitting at λ =8.36 μm and with anti-waveguides formed by high refraction index contrast ($\Delta = 0.08-0.12$) has shown that it is possible to attain resonant leaky-wave coupling for phase-locked arrays which can provide stable in-phase -mode array operation [71]. It is essential that the output beam was near-diffraction-limited and was of 5.5 W peak power at pulse operation. It has been concluded that resonant leaky-wave coupling of QCLs bringing about the in-phase mode operation can be expected only in the case of designs that are composed of leaky-waveguides (or anti-waveguides) [71]. Only then the wave coupling restricts the side modes and at resonance, this provides a stable work of the lasers although the emission has multiple peaks. The whole process has been termed "phase-locking" and requires a very complicated structure of the arrays. Then, because ~4.5 μm wavelength is so important in practice, new resonant leaky-wave-coupled QCL phase-locked arrays emitting at 4.7 μm have been fabricated. Details of the improved structure are described in Ref. 72 and Figure 7 presents a sketch of three elements of the array. The inter-element region width can be edged to attain the resonant-coupling condition. The QCL arrays operated in the regime of near-resonant leaky-wave coupled and emitted up to 3.6 W pulsed power with a near-diffraction limited (<1.7 times) beam pattern. Improvements of this type of arrays led recently to 5.1 W with slightly better beam quality (1.6 times diffraction limited) [73].

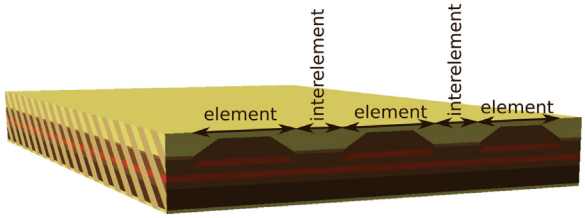

Fig. 7. Configuration principle of a phase-locked QCL array (based on idea presented in Ref. 71).

It is believed that by scaling the number of the array elements these devices hold potential for reaching output power of 10 W in the near-diffraction limited beams [72]. Leaky-wave-coupled phase-locked arrays have also potential CW operation with multi-watt-range output power [74].

3.2. Internally uncoupled multi-wavelength DFB QCL arrays

The idea of arranging DFB QC lasers in form of laser bars was simply a step forward towards increasing their output power as it was in the case of diode lasers. However, the new array configurations were based on a DFB feedback, and each QCL laser could have a grating of different period [75]. That feature with an opportunity of individual current supplying each laser in the array has allowed for wide tuning of narrow linewidth beams [76]. The mentioned QCL arrays operated at a wavelength of 9.5 μm and their beams could be combined to increase the radiance as described below.

Continuation of the effort brought QCL MOPA array structures [77,78]. The arrays in question formed an array of 16 or more QCL MOPA devices. Each of them comprised two sections: a narrow ridge DFB laser that functioned as the master oscillator and a tapered power amplifier (PA). Each DFB laser in the array had a grating of a different period in order to achieve a different emission wavelength. Proper antireflection coatings were applied to PA section allowing for strong optical amplification in single pass travelling wave configuration. Lasers were pulse operated and displayed high power (above 4 W) in single lobe peaks within the wavelength band from 9.2–9.8 μm. The individual current supply of the array element allowed for independent addressing of different wavelengths. The far-field single-lobed beam characteristics measured in plane showed an average FWHM angle of 7.7°.

3.3. Multi-wavelength high power MOPA QCL arrays

The idea presented in Ref. 76 has been significantly improved by employing arrays formed from QCLs of the MOPA-taper configurations with all advantages of these lasers described above. Detailed features of that MOPA arrays have been described in an excellent review paper by P. Rauter and F. Capasso cited previously in the introduction [9], as well as [77,78]. The configuration of that array is shown in Fig. 8. It should be noticed that DFB seeds are isolated from the taper power amplifier and therefore independently current supplied.

It is worthwhile to mention here that mentioned high-power MOPA QCL arrays were capable to generate beams of up to 10 W

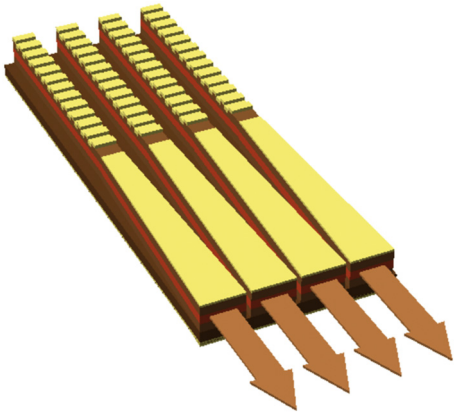

Fig. 8. Configuration of MOPA-taper QCL array (based on Refs. 77 and 78).

peak power in the single-mode pulse operation, although it should be emphasised that the beams of the individual lasers were not be combined. They could work at 14 different wavelengths that could be rapidly switched with a frequency of 100 kHz.

Summing up: it is believed that this type of QCL arrays, being in addition compact and electrically tunable have the potential to outperform the external cavity laser (ECL) systems in spectroscopy.

4. Beam combining as a way to increasing radiance of QCLs arrays

Scaling up the laser array radiance requires first of all collimation of the laser array beams. However, these beams even if collimated, still will be affected by the presence of many wavelengths limited by the gain emission spectrum of the individual lasers in the array and that causes detrimental interference. In addition, each beam is radially asymmetrical. This results in a large difference between values of the BPP_f and BPP_s where f and s stand for the planes adequately parallel and perpendicular to the epi laser layers. A solution to this problem is synchronization of the array sub-beams by external optics that forms external cavity lasers. Such technique is termed beam combining to underline the fact that we deal with the beams already radiating outside the lasers. It turned out to be efficient and has become a subject of intensive investigations [79]. It is worthwhile to notice that, in fact, this is another approach to scaling up the radiance.

A similar attempt, but restricted to the interior of the laser array is in fact realized in resonant leaky-wave coupled phase-locked arrays described above, but is limited by inter-dimensions of the array in comparison with the emitted wavelengths. The prevailing majority of beam combining experiments concerned diode laser bars since they were available a long time before QCL arrays technology matured enough to make them useful for beam multiplication *via* integration of the QCLs into a form of arrays and subsequent optical combining would lead, in an ideal case, to synchronization of the individual beams and thus to multiplication of the output beam radiance. By synchronization, we understand that output beams contain waves of the same wavelength, phase and direction. Such procedure is termed Coherent Beam Combining (CBC). In practice, however, phase synchronization is difficult to achieve. Therefore, a technique of non-coherent synchronization has been proposed which means putting into an order propagation direction of the individual beams so they cannot interfere. Such operation is termed Wavelength Beam Combining (WBC) or Spectral Beam Combining (SBC). Both techniques CBC and WBC have been investigated for years and found numerous applications including infrared counter-measure (IRCM) systems. They have been described in many excellent papers among them by T.Y. Fan [26]. The experiments were carried out using diode laser bars since these were available a long time before QCL arrays technology matured enough to make them useful for the beam combining systems.

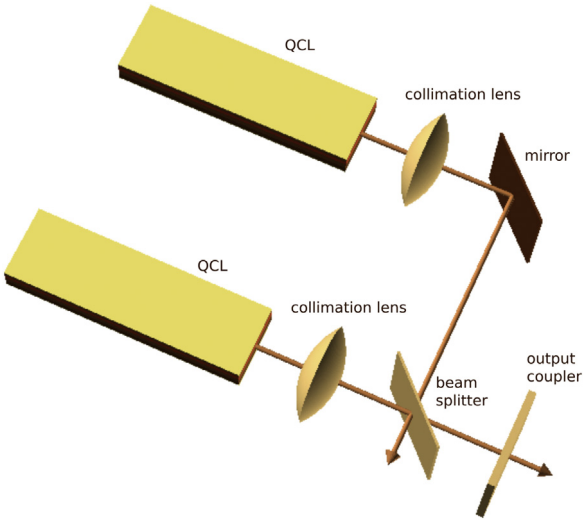

Fig. 9. The Michelson cavity setup displaying an idea of the Coherent Beam Combining (after Ref. 80).

4.1. Coherent beam combining (CBC)

4.1.1. CBC presented with aid of the Michelson cavity

According to the definition of the CBC process, lasers arranged in the array should emit waves of the same length and phase controlled up to a fraction of 2π. The constructive interference in the far field is possible only in that case. Coherent synchronization of QCL arrays is complicated because of material non-uniformity along the array and nonlinear processes taking place under high currents that supply the neighbouring lasers. All these difficulties may be overcome by employing the discussed below methods. They require, however, optical systems that include selective wavelength filtration and thus form an external cavity (EC) laser. A number of coherent beam combining concepts have been studied to push forward performance of QCL array systems. The simplest approach leading to CBC may be based on exploiting the principle of the Michelson cavity [80] as displayed in Fig. 9.

The optical system consists of two QCLs, a collimation lens, a mirror, a beam splitter (50/50) and an output coupler (R = 30%). The back laser facets are AR (R = 2%) coated. Both lasers emit TM polarized beams due to their intersubband principle of operation. The common cavity optical system combined with the extorted oscillation on the laser mode with the lowest threshold results in phase-locking between them. The process can be affected by changes of the currents supplying the lasers or distances between the elements in the common cavity. The efficiency of wave combining depends on many factors but can be as high as 85%.

The experiments had shown that spectral characteristics of the output beam display a narrow single lobe. Coupling of the waves in the common cavity has led to domination of the in-phase modes that left the system through the output coupler. Presence of many longitudinal modes excited within the gain range of each QCLs had simplified the competition. The obtained values of the M^2 factor were $M_x{}^2$<1.2 and $M_y{}^2$<1.4 and. thus they were very close to the values measured for individual QCLs. Unfortunately, the whole system was fund to be rather unstable and sensitive to changes in the supply current. Consequently, this observation and lack of scalabil-

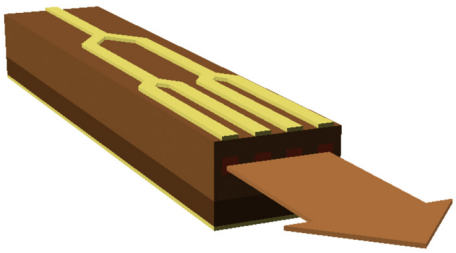

Fig. 10. Idea of the "Y junction" coherent beam combining (based on idea presented in Ref. 83).

ity make these ideas more interesting from the point of view of the phenomena than practical.

4.1.2. CBC in the Y-junctions tree arrays

Phase locking of laser beams has also been achieved in a two-branch Y-type resonator (termed elsewhere "Y-junction") where the suppression of higher order lateral modes leads to a stable super-mode operation. The Y-junction showed low coupling losses and in-phase operation with diffraction limited divergence. Such phase locking has been already demonstrated for diode laser bars. Applied to QCLs has brought the phase locking where one of the of higher order lateral waveguide modes leads to a stable super-mode operation [81,82]. The concept yields promising results in terms of power scaling efficiency. In the super-mode approach even if a coupled array is composed of elements of different optical path length, the optical spectrum is expected to reach self-adjustment in order to minimize the overall loss of the resonator. In this respect, more than two branches can be combined in parallel in the same manner by means of several Y-junctions. As the outcome, we have so-called "tree array QCL". A principle of that array configuration is shown in Fig. 10 [83].

An output power of 1.5 W CW RT was demonstrated for four-branch QCL arrays utilizing the Y-junction design [83]. The out-of-phase modes have to be further suppressed for BH QCL tree arrays with a large number of merges to achieve along the axis a diffractive-limited beam in a form of a stem. All the elements are single-mode waveguides that are uniformly pumped. They merge together at the back facet. This ensures parallel coupling between the elements leads to an on-axis far-field intensity distribution with nearly diffraction-limited divergence. Radiance of the ridge waveguide QCLs did not exceed that for single emitters, primarily because the power does not scale with the number of elements. This was due to modal competition among branches of different length. This problem was dealt with by using multimode interferometers instead of Y-junctions [84]. Such an array of 8 lasers emitted 15 W in pulse operation, which is 5 times more than a single laser.

4.1.3. External cavity QCLs with Dammann gratings

A very sophisticated, although difficult to implement solution leading to CBC is based on the external cavity principle with a dispersion grating of a special type called a binary dispersion grating (known also as Dammann grating) [85].

The grating is of a specific profile with two different periods as shown in Fig. 11. Its purpose is to generate strong diffraction orders with approximately the same amplitude. They should appear in number N equal to the number of the lasers participating in the summarizing process. The other diffractive orders should be weak *i.e.* containing low power. The efficiency of the beams dispersion, defined as the ratio of the power contained in the N demanded orders to the total beam power falling on the grating is maximized by appropriate adjusting of the grating profile. This can be done with an aid of advanced optimization techniques. Combining efficiency of 66% has been achieved for 5 laser Dammann grating

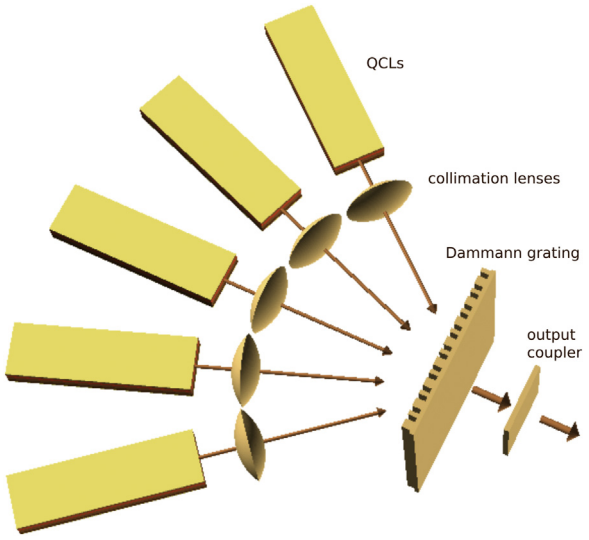

Fig. 11. External Cavity QCL system with binary dispersion grating [based of idea presented in Ref. 85.

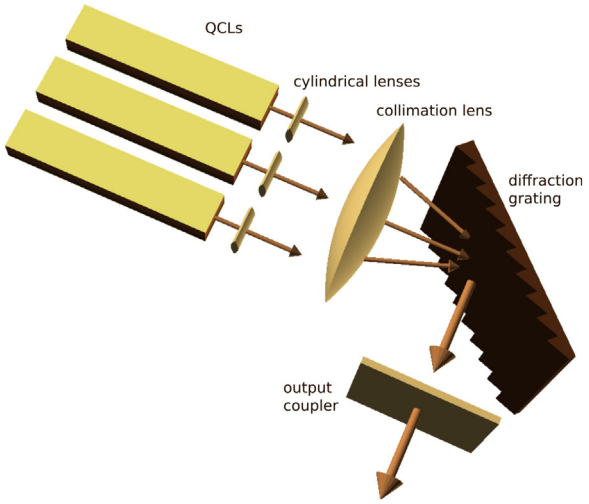

Fig. 12. Typical structure of the.

system [85]. What is more important, however, the output beam was nearly diffraction limited and $M_x^2 < 1.2$ and $M_y^2 < 1.6$ for slow and fast axis, respectively, were measured.

Despite the excellent results, the systems with Dammann gratings did not gain practical importance mainly due to difficulties encountered in the process of the grating design and manufacturing.

4.2. Non-coherent beam combining (WBC)

4.2.1. External cavity systems in Littman configuration

A non-coherent beam combining termed Wavelength Beam Combining (WBC) has on purpose to increase spatial radiance of the summed up beams emitted by lasers in an array without changing their spectral radiance. Described in the literature experiments leading to WBC have been exploiting the external cavity design concept and a plethora of circuits containing various type filters, external mirrors with spatially variable reflection or phase coefficients. Most successful, however, turned out the application of diffraction gratings operating in systems based on the so-called "Littman configuration". The principle of such system is sketched in Fig. 12. Details of the experimental optical systems shown there

may be different depending on the assumed purpose of investigation. The idea has been first exploited by applying diode laser bars [86]. Detailed description and properties of these devices can be found in Refs. 87–89. The concept was soon followed by its adoption to QCL arrays [90].

Optical system sketched in Fig. 12 forms a resonant cavity created by the back lasers facets coated with reflective layers and the semi-reflecting output mirror. The front lasers facets have been AR (anti-reflective) coated (around 0.2%) to avoid internal reflections in the system and the related losses. The optical feedback is secured for the waves of different lengths that fall on the grating at the angle selected by the semi-reflecting mirror that closes the resonant cavity. This geometry resembles Littman configuration but is in a way specific since the grating angle is adjusted to obtain only the 1st order diffraction to avoid efficiency losses to higher diffraction orders. The beams emitted by individual lasers of the array are naturally divergent. Cylindrical AR coated lenses are therefore used to make them parallel in the fast axis. Their divergence in the slow axis is partly eliminated by an aspheric lens used to concentrate them on the grating and to transform the position of each elementary beam into incidence angle of the grating. The local offset between the positions of the individual lasers and the elementary beams relative to the position of the central laser must be compensated by the grating and semi-reflecting output mirror. The main purpose of the grating is not to select out a specific wavelength but to select waves that propagate in the same direction. System designed for beam combining based on the Littman configuration.

Since emission of the QCL's beams is polarized perpendicularly to the laser layer growth direction, and efficiency of the grating may be higher for in-plane polarization. In that case, an additional antireflection coated $\lambda/2$ may be inserted into the optical path to rotate the polarization by 90°. Summing up, the external cavity selects different wavelengths for all array elements as needed to force coaxial propagation.

Most important in the WBC technique become properties of the optical system that decides about the wall-plug efficiency of the whole arrangement. The AR coatings mentioned above become very important as all parasitic reflections of the uncontrolled higher order mode generation cause decrease of the system efficiency. Perhaps even more important is the efficiency of the diffraction grating which depends on many factors like the cross-section profile, period and polarization of the coupled waves. The QCLs emit TM polarized light, therefore, grating efficiency for that direction should be taken into account. Mathematical designing necessary to optimize diffraction gratings for the particular WBC system turned out to be complicated and, in practice, it remains to rely on empirical adjustments.

The total output power of the combining system is up to certain limits proportional to the number of lasers in the array. The total efficiency of the combining process is of the order of 50% [91] and the output contains many wavelengths. Nevertheless, the described type of arrays operating at 4.6 μm wavelength was characterized by M^2<2 for both slow and fast axes. Thus, for the output peak power of 30 W, one may estimate the radiance to be of the order of 35.4 MW cm^{-2} sr^{-1}.

Typical QCL arrays may be tuned directly in the WBC systems by adjusting the position of the grating. Their general disadvantage is the necessity to make the system mechanically stable and resistant to shocks. The obtained linewidth is not sufficiently low for applications in spectroscopy.

4.2.2. *DFB QCL arrays exploited in the ECL configuration*

The QCL arrays composed of the DFB type lasers open up a plethora of new possibilities resulting from the numerous advantages of these lasers. One of them, proposed in Ref. 76 was based on an application of DFB QCL arrays composed of lasers with different DFB frequency. Signals emitted by these arrays were optically combined by overlapping in a Littrow-like system. To improve its radiance a second grating was afterwards added making it more Littman-like [90]. In this paper the radiance is substituted by "beam quality" calculated using a times-diffraction–limited (TDL) metric for Gaussian given by $\frac{\pi W\theta}{4\lambda}$ where W is the full-width FW 1/e^2 near field size, θ is the FW 1/e^2 far-field divergence. The beam quality 1.4 total diffraction limit (TDL) to 1.7 TDL has been measured. Many more details can be found in Ref. 90.

The described above ECL systems delivered interesting results, but these systems were mechanically complicated and not always operated at the expected power efficiency. A question arises what could be expected if each laser in the array was equipped with its own lens. The answer can be found in Ref. 91. A system was built in which a micro-lens array was placed exactly in front of the QCL linear array operating within λ = 4.5–5 μm range of wavelengths. The lenses were made of silicon, had the same 500 μm pitch as the QCLs and were placed in the distance of 100 μm from the laser facets. It was found that the total output power of the array was very close to the summarized power of the individual lasers and the beam had the form of a single lobe. But in the lateral direction, the value of its $M_x{}^2$ factor was around 30 which mean that a special additional phase adjusting system should be built to secure an effective beam combining.

5. Summary and conclusions

Described beam combining systems, both CBC and WBC, proved to be so far the best optical arrangement for the QCL arrays capable of delivering high output power beams with relatively high spatial radiance. In particular, the external cavity configuration brings currently the best solutions when both high power (radiance) and wide tuning range are necessary. The record high tuning ranges have been obtained when following this approach. Unfortunately, a general disadvantage of all external cavity systems is the necessity to apply precise, sophisticated and reliable optomechanical systems.

Shown below Table 1 has been composed to visualize described in the literature results that provoked writing this paper. Frequent lacking of M^2 values in the quoted literature makes the radiance values indicated in some places of the text doubtful, but at least they give an idea about a magnitude of this parameter. The table has been set up chronologically to show the progress and hopes for future developments but these are rather disappointing, at least after studies of the publically accessible literature.

Radiance is a QCL's beam parameter that depends on the laser output power and the beam quality. This is why this parameter is of particular importance when we are describing properties of semiconductor lasers, in particular, QCLs or their arrays designed for long distance applications. Beams emitted by these devices may be very much different from the Gaussian ones and this feature is very often confused with that intuitively associated with beams of other lasers. Relatively poor beam properties of QCLs arrays demonstrated by high values of the M^2 factor might, unfortunately, discriminate them from the applications that demand beams of the very high radiance.

CRediT authorship contribution statement

B. Mroziewicz: Conceptualization, Data curation, Investigation, Resources, Supervision, Writing – original draft. **E. Pruszyńska-Karbownik:** Validation, Visualization, Writing – review & editing.

Acknowledgements

The authors gratefully acknowledge valuable discussions with prof. M. Bugajski of the Institute of Electron Technology. This work

was supported under Grant No DOB1-6/1/PS/2014 by The National Centre for Research and Development in Poland.

References

[1] J. Faist, F. Capasso, D.L. Sivco, C. Sirtori, A.L. Hutchinson, A.Y. Cho, Quantum cascade laser", Science 264 (1994) 553–556.
[2] J. Devenson, R. Teissier, O. Cathabard, A.N. Baranov, InAs/AlSb quantum cascade lasers emitting below 3 μm, Appl. Phys. Lett. 90 (2007), 111118.
[3] J.A. Fan, M.A. Belkin, F. Capasso, S.P. Khanna, M. Lachab, A.G. Davies, E.H. Linfield, Wide-ridge metal-metal terahertz quantum cascade lasers with high-order lateral mode suppression, Appl. Phys. Lett. 92 (2008), 031106.
[4] M.A. Belkin, F. Capasso, F. Xie, A. Belyanin, M. Fischer, A. Wittmann, J. Faist, Room temperature terahertz quantum cascade laser source based on intracavity difference-frequency generation", Appl. Phys. Lett. 92 (2008) 201101.
[5] R.F. Curl, F. Capasso, C. Gmahl, A.A. Kosterev, B. McManus, R. Lewicki, M. Pusharsky, G. Wysocki, F.K. Tittel, Quantum cascade lasers in chemical physics, Chem. Phys. Lett. 487 (2010) 1–18.
[6] R. Centeno, D. Marchenko, J. Mandon, S.M. Cristescu, G. Wulterkens, F.J.M. Harren, High power, widely tunable, mode-hop free, continuous wave external cavity quantum cascade laser for multi-species trace gas detection, Appl. Phys. Lett. 105 (2014), 261907.
[7] A. Lyakh, R. Maulini, A.G. Tseokun, C. Kumar, N. Patel, Progress in high-performance quantum cascade lasers, Opt. Eng. 49 (11) (2010), 111105.
[8] R.M. Williams, J.F. Kelly, J.S. Hartman, S.W. Sharpe, M.S. Taubman, J.L. Hall, F. Capasso, C. Gmachl, D.L. Sivco, J.N. Baillargeon, A.Y. Cho, Kilohertz linewidth from frequency-stabilized mid-infrared quantum cascade lasers, Opt. Lett. 24 (24) (1999) 1844–1846.
[9] P. Rauter, F. Capasso, Multi -wavelength quantum cascade laser arrays, Laser Photon. Rev. 9 (5) (2015) 452–477.
[10] M. Razeghi, Q.Y. Lu, N. Bandyopadhyay, W. Zhou, D. Heydari, Y. Bai, S. Slivken, Quantum cascade lasers: from tool to product, Opt. Express 23 (7) (2015) 8462–8475.
[11] A. Bismuto, St. Blaser, R. Terazzi, T. Gresch, A. Muller, High performance, low dissipation quantum cascade lasers across the mid-IR range, Opt. Express 23 (4) (2015) 5477–5484.
[12] M. Troccoli, High-power emission and single-mode operation of quantum cascade lasers for industrial applications, IEEE J. Sel. Top. Quant. Electron. 21 (6) (2015), 1200207.
[13] M.S. Vitiello, G. Scalari, B. Williams, P. De Natale, Quantum cascade lasers: 20 years of challenges, Opt. Express 23 (4) (2016) 5167–5172.
[14] P. Shukla, J. Lawrence, Y. Zhang, Understanding laser beam brightness: a review and new prospective in material processing, Opt. Laser Technol. 75 (2015) 40–51.
[15] M. Trocolli, D. Bour, S. Corzine, G. Höfler, A. Tandon, D. Mars, D.J. Smith, L. Diehl, F. Capasso, Low-threshold continuous-wave operation of quantum-cascade lasers grown by metalorganic vapour phase epitaxy, Appl. Phys. Lett. 85 (24) (2004) 5842.
[16] F. Capasso, High-performance mid-infrared quantum cascade lasers, Opt. Eng. 49 (11) (2010), 111102-1.
[17] M. Razeghi, N. Bandyopadhyay, Y. Bai, Q. Lu, S. Slivken, Recent advances in mid infrared (3-5μm) Quantum Cascade Lasers, Opt. Mater. Express 3 (11) (2013) 1872.
[18] D. Botez, J.D. Kirch, C. Boyle, K.M. Oresick, C. Sigler, H. Kim, Y.V. Flores, High-efficiency, high-power mid-infrared quantum cascade lasers [Invited], Opt. Mater. Express 8 (5) (2018) 1378–1398.
[19] D. Botez, C.C. Chang, L.J. Mawst, Temperature sensitivity of the electro-optical characteristics for mid-infrared (λ = 3-16 μm)-emitting quantum cascade lasers", J. Phys. D Appl. Phys. 49 (4) (2015), 043001.
[20] M. Lindskog, J.M. Wolf, V. Trinite, V. Liverini, J. Faist, G. Maisons, A. Wacker, Comparative analysis of quantum cascade laser modeling based on density matrices and non-equilibrium Green's functions, Appl. Phys. Lett. 105 (10) (2014) 0–5.
[21] M. Bugajski, P. Gutowski, P. Karbownik, A. Kolek, G. Hałdaś, K. Pierściński, D. Pierścińka, J. Kubacka-Traczyk, I. Sankowska, A. Trajnerowicz, K. Kosiel, A. Szerling, J. Grzonka, K. Kurzydłowski, T. Slight, W. Meredith, Mid-IR quantum cascade lasers: device technology and non-equilibrium Green's function modelling of electro-optical characteristics, Phys. Status Solidi B 251 (6) (2014) 1144–1157.
[22] A. Kolek, G. Hałdaś, M. Bugajski, K. Pierściński, Piotr Gutowski, Impact of injector doping on threshold current of mid-infrared quantum cascade laser–Non-Equilibrium green's function analysis", IEEE J. Sel. Top. Quant. Electron. 21 (1) (2015), 1200110.
[23] A.E. Siegman, Defining, measuring, and optimizing laser beam quality, SPIE (1868) 2–12.
[24] M.W. Sasnett, T.F. Johnston Jr., Beam characterization and measurement of propagation attributes, SPIE 1414, Laser Beam Diagnostics (1991) 21–32.
[25] EN ISO 11146-2:2005, Lasers and Laser-related Equipment - Test Methods for Laser Beam Widths, Divergence Angles and Beam Propagation Ratios - Part 2: General Astigmatic Beams, 2005.
[26] T.Y. Fan, Laser beam combining for high-power high-radiance sources", IEEE J. Sel. Top. Quantum Electron. 11 (3) (2005) 567–577.
[27] K. Krishnaswami, B.E. Bernacki, B.D. Cannon, N. Ho, N.C. Anheier, Emission and propagation properties of midinfrared quantum cascade lasers, IEEE Photon. Technol. Lett. 20 (4) (2008) 306–308.
[28] R. Maulini, A. Lyakh, A. Tsekoun, R. Go, Ch. Pflügl, L. Diehl, F. Capasso, C. Kumar, N. Patel, High power thermoelectrically cooled and uncooled quantum cascade lasers with optimized reflectivity facet coatings, Appl. Phys. Lett. 95 (2009), 151112.
[29] D. Pierścińska, P. Gutowski, G. Hałdaś, A. Kolek, I. Sankowska, J. Grzonka, J. Mizera, K. Pierściński, M. Bugajski, Above room temperature operation of InGaAs/AlGaAs/GaAs quantum cascade lasers, Semicond. Sci. Technol. 33 (2018), 035006.
[30] Y. Bai, S.R. Darvish, N. Bandyopadhyay, S. Slivken, M. Razeghi, Optimizing facet coating of quantum cascade lasers for low power consumption, J. Appl. Phys. 109 (2011), 035006.
[31] A. Lyakh, P. Zory, D. Wasserman, G. Shu, C. Gmachl, M. D'Souza, D. Botez, D. Bour, Narrow stripe-width, low-ridge high power quantum cascade lasers, Appl. Phys. Lett. 90 (2007), 141107.
[32] A. Evans, S.R. Darvish, S. Slivken, J. Nguyen, Y. Bai, M. Razeghi, Buried heterostructure quantum cascade lasers with high continuous-wave wall plug efficiency, Appl. Phys. Lett. 91 (2007), 071101.
[33] Y. Bai, N. Bandyopadhyay, S. Tsao, E. Selcuk, S. Slivken, M. Razeghi, Highly temperature insensitive quantum cascade lasers, Appl. Phys. Lett. 97 (2010), 251104.
[34] A. Lyakh, R. Maulini, A. Tsekoun, R. Go, C. Pflugl, L. Diehl, Q.J. Wang, F. Capasso, C. Kumar, N. Patel, 3 W continues-wave room temperature single-facet emission from quantum cascade lasers based on non-resonant extraction design approach, Appl. Phys. Lett. 95 (2009), 141113.
[35] A. Lyakh, C. Pflügl, L. Diehl, Q.J. Wang, F. Capasso, X.J. Wang, J.Y. Fan, T. Tanbun-Ek, R. Maulini, A. Tsekoun, R. Go, C. Kumar, N. Patel, 1.6W high wall plug efficiency, continuous-wave room temperature quantum cascade laser emitting at 4.6μm, Appl. Phys. Lett. 92 (2008) 111110.
[36] J.C. Shin, M. D'Souza, Z. Liu, J. Kirch, L.J. Mawst, D. Botez, I. Vurgaftman, J.R. Meyer, Highly temperature insensitive, deep-well 4.8 μm emitting quantum cascade semiconductor lasers, Appl. Phys. Lett. 94 (20) (2009) 2007–2010.
[37] Y. Bai, N. Bandyopadhyay, S. Tsao, S. Slivken, M. Razeghi, Room temperature quantum cascade lasers with 27% wall plug efficiency, Appl. Phys. Lett. 98 (2011), 181102.
[38] F. Xie, C. Caneau, H.P. Leblanc, N.J. Visovsky, S.C. Chaparala, O.D. Deichmann, T. Day., "Room temperature CW operation of short wavelength quantum cascade lasers made of strain balanced $Ga_xIn_{1-x}As/Al_yIn_{1-y}As$ material on InP substrates, IEEE J. Sel. Top. Quantum Electron. 17 (2011) 1445–1452.
[39] Y. Bai, S. Slivken, S.R. Darvish, A. Haddadi, B. Gökden, M. Razeghi, High power broad area quantum cascade lasers, Appl. Phys. Lett. 95 (2009), 221104.
[40] M.P. Semtsiv, W. Masselink, Above room temperature continuous wave operation of a broad-area quantum-cascade laser, Appl. Phys. Lett. 109 (2016), 203502.
[41] I. Sergachev, R. Maulini, A. Bismuto, S. Blaser, T. Gresch, A. Muller, Gain-guided broad area quantum cascade lasers emitting 23,5 W peak power at room temperature, Opt. Express 24 (17) (2016) 19063–19071.
[42] A. Tsekoun, R. Go, M. Pushkrsky, M. Razegi, C. Kumar, N. Patel, Improved performance of quantum cascade lasers through a scalable, manufacturable epitaxial-side-down mounting process, PNAS 103 (13) (2006) 4831–4835.
[43] C.A. Evans, V.D. Jovanović, D. Indjin, Z. Ikonić, P. Harrison, Investigation of thermal effects in quantum-cascade lasers, IEEE J. Quant. Electron. 42 (9) (2006) 859–861.
[44] L. Missaggia, Ch. Wang, M. Connors, B. Saar, A. Sanchez-Rubio, K. Creedon, G. Turner, W. Herzog, Thermal management of quantum cascade lasers in an individually addressable monolithic array architecture, SPIE 9730 (2016), 973008-1.
[45] D. Pierścińska, K. Pierściński, M. Morawiec, P. Karbownik, P. Gutowski, M. Bugajski, CCD thermoreflectance spectroscopy as a tool for thermal characterization of quantum cascade lasers, Semicond. Sci. Technol. 31 (2016), 115006.
[46] D. Pierścińska, Thermoreflectance spectroscopy-Analysis of thermal processes in semiconductor lasers, J. Phys. D Appl. Phys. 51 (2018), 013001.
[47] Q. Yang, M. Kinzer, F. Fuchs, S. Hugger, B. Hinkov, W. Bronner, R. Lösch, R. Aidam, J. Wagner, Beam steering and lateral hole burning in mid-infrared quantum-cascade lasers, Phys. Status Solidi (c) 9 (2) (2012) 302–305.
[48] Q.Y. Lu, Y. Bai, N. Bandyopadhyay, S. Slivken, M. Razeghi, 2.4 W room temperature continuous wave operation of distributed feedback quantum cascade lasers, Appl. Phys. Lett. 98 (2011) 81106.
[49] C. Gmachl, A. Straub, R. Colombelli, F. Capasso, D.L. Sivco, A.M. Sergent, A.Y. Cho, Single-mode, tunable distributed-feedback and multiple-wavelength quantum cascade lasers, IEEE J. Quant. Electron. 38 (6) (2002) 569.
[50] B.G. Lee, M.A. Belkin, R. Audet, J. MacArthur, L. Diehl, Ch. Pflügl, F. Capasso, Widely tunable single-mode quantum cascade laser source for mid-infrared spectroscopy, Appl. Phys. Lett. 91 (2007), 231101.
[51] S. Slivken, N. Bandyopadhyay, S. Tsao, S. Nida, Y. Bai, Q.Y. Lu, M. Razeghi, Sampled grating, distributed feedback quantum cascade lasers with broad tunability and continuous operation at room temperature, Appl. Phys. Lett. 100 (2012), 261112.
[52] R. Centeno, D. Marchenko, J. Mandon, S.M. Cristescu, G. Wulterkens, F.J.M. Harren, High power, widely tunable, mode-hop free, continuous wave external cavity quantum cascade laser for multi-species trace gas detection, Appl. Phys. Lett. 105 (2014) 261907.

[53] S. Ahn, C. Schwarzer, T. Zederbauer, D.C. MacFarland, H. Detz, A.M. Andrews, W. Schrenk, G. Strasser, High-power, low-lateral divergence broad area quantum cascade lasers with a tilted front facet, Appl. Phys. Lett. 104 (2014) 105110.
[54] Y. Bai, S. Slivken, Q.Y. Lu, N. Bandyopadhyay, M. Razeghi, Angled cavity broad area quantum cascade lasers, Appl. Phys. Lett. 101 (2012), 081106.
[55] D. Heydari, Y. Bai, N. Bandyopadhyay, S. Slivken, M. Razeghi, High brightness angled cavity quantum cascade lasers", Appl. Phys. Lett. 106 (2015), 091105.
[56] C. Boyle, C. Sigler, J.D. Kirch, D.F. Lindberg, T. Earles, D. Botez, J. Mawst, High-power, surface-emitting quantum cascade laser operating in a symmetric grating mode, Appl. Phys. Lett. 108 (2016) 121107.
[57] M. Trocolli, C. Gmachl, F. Capasso, D.L. Sivco, A.Y. Cho, Mid-infrared (λ=7.4 μm) quantum cascade laser amplifier for high power single-mode emission and improved beam quality, Appl. Phys. Lett. 80 (2002) 4103.
[58] B. Hinkov, M. Beck, E. Gini, J. Faist, Quantum cascade laser in a master oscillator power amplifier configuration with Watt-level optical output power, Opt. Express 21 (16) (2013) 19180–19186.
[59] L. Nähle, J. Semmel, W. Kaiser, S. Höfling, A. Forchal, Tapered quantum cascade lasers, Appl. Phys. Lett. 91 (2007), 181122.
[60] A. Lyakh, R. Maulini, A. Tsekoun, R. Go, C. Kumar, N. Patel, Tapered 4.7 μm quantum cascade lasers with highly strained active region composition delivering over 4.5 watts of continuous wave optical power, Opt. Express 20 (4) (2012) 4382–4388.
[61] P. Rauter, S. Menzel, B. Gokden, A.K. Goyal, Ch.A. Wang, A. Sanchez, G. Turner, F. Capasso, Single-mode tapered quantum cascade lasers, Appl. Phys. Lett. 102 (2013), 181102.
[62] S. Menzel, L. Diehl, C. Pflügl, A. Goyal, C. Wang, A. Sanchez, G. Turner, F. Capasso, Quantum cascade laser master-oscillator power-amplifier with 1.5 W output power at 300 K, Opt. Express 19 (17) (2011) 16229–16235.
[63] M. Sakowicz, E. Pruszynska-Karbownik, A. Kuzmicz, K. Janus, P. Gutowski, K. Michalak, Mid-infrared quantum cascade lasers with nonuniformly tapered waveguides, J. Light. Technol. 37 (10) (2019) 2324–2327.
[64] B. Gökden, T.S. Mansuripur, R. Blanchard, Ch. Wang, A. Goyal, A. Sanchez-Rubio, G. Turner, F. Capasso, "High-brightness tapered quantum cascade lasers, Appl. Phys. Lett. 102 (2013), 053503.
[65] R. Blanchard, T.S. Marisuripur, B. Gökhden, N. Yu, M. Kats, P. Genevet, K. Fujita, T. Edamura, M. Yamanishi, F. Capasso, High-power low-divergence tapered quantum cascade lasers with plasmonic collimators, Appl. Phys. Lett. 102 (2013), 191114.
[66] B. Gökden, Y. Bai, N. Bandyopadhyay, S. Slivken, M. Razegi, "Broad area photonic crystal distributed feedback quantum cascade lasers emitting 34 W at λ4.36 μm, Appl. Phys. Lett. 97 (2010), 131112.
[67] D. Botez, L. Mawst, G. Peterson, T.J. Roth, Phase - locked arrays of antiguides: modal content and discrimination, IEEE J. Quant. Electron. 26 (3) (1990) 482–495.
[68] R.F. Nabiev, D. Botez, Comprehensive above -Threshold analysis of antiguided diode laser arrays, IEEE J. Sel. Top. Quant. Electron. 1 (2) (1995) 138–149.
[69] R. Colombelli, K. Srinivasan, M. Trocolli, O. Painter, C.F. Gmachl, D.M. Tennant, A.M. Sergent, D.L. Sivco, A.Y. Cho, F. Capasso, Quantum cascade surface-emitting photonic crystal laser", Science 302 (21) (2003) 1374.
[70] C. Sigler, J.D. Kirch, L.J. Mawst, Z. Yu, D. Botez, Design for high power, single-lobe, grating-surface-emitting quantum cascade lasers, Appl. Phys. Lett. 104 (2014) 131108.
[71] J.D. Kirch, C.C. Chang, C. Boyle, L.J. Mawst, D. Lindberg III, T. Earles, D. Botez, 5.5 W near-diffraction-power from resonant leaky wave coupled phase-locked arrays of quantum cascade lasers, Appl. Phys. Lett. 106 (2015), 061113.
[72] C. Sigler, C.A. Boyle, J.D. Kirch, D. Lindberg III, T. Earles, D. Botez, L.J. Mawst, 4.7 μm -Emitting near-resonant leaky wave-coupled quantum cascade laser phase-locked arrays, IEEE J. Sel. Top. Quantum Electron. 23 (6) (2017), 1200706.
[73] L.J. Mawst, C. Sigler, C. Boyle, J.D. Kirch, K. Oresick, H. Kim, D. Lindberg, T. Earles, D. Botez, High power MOCVD-grown quantum cascade lasers, in: Proc. 31 IEEE Photonics Conference (IPC), 2018.
[74] C. Sigler, C. Chang, J.D. Kirch, L.J. Mawst, D. Botez, T. Earles, Design of resonant leaky-wave coupled phase-locked arrays of Mid-IR quantum cascade lasers, IEEE J. Sel. Top. Quant. Electron. 21 (6) (2015), 1200810.
[75] B.G. Lee, M.A. Belkin, Ch. Pflügl, L. Diehl, H.A. Zhang, R.M. Audet, J.Mac Arthur, D.P. Bour, S.W. Corzine, G.E. Höfler, F. Capasso, DFB quantum cascade laser arrays, IEEE J. Quant. Electron. 45 (5) (2009) 554–565.
[76] B.G. Lee, J. Kansky, A.K. Goyal, Ch. Pflügl, L. Diehl, M.A. Belkin, A. Sanchez, F. Capasso, "Beam combining of quantum cascade laser arrays, Opt. Express 17 (18) (2009) 16216–16224.
[77] P. Rauter, S. Menzel, A.K. Goyal, Ch.A. Wang, A. Sanchez, G. Turner, F. Capasso, High-power arrays of quantum cascade laser master-oscillator power-amplifiers", Opt. Express 21 (4) (2013) 4518–4530.
[78] P. Rauter, S. Menzel, A.K. Goyal, B. Gökden, C.A. Wang, A. Sanchez, G.W. Turner, F. Capasso, Master-oscillator power-amplifier quantum cascade laser array, Appl. Phys. Lett. 101 (2012), 261117.
[79] Y. Liu, Y. Braiman, "Synchronization of high-power broad-area semiconductor lasers, J. Sel. Top. Quant. Electron. 10 (5) (2004) 1013–1024.
[80] G. Bloom, Ch. Larat, E. Lallier, M. Carras, X. Marcadet, Coherent combining of two quantum cascade lasers in a Michelson cavity, Opt. Lett. 35 (11) (2010) 1917–1919.
[81] L.K. Hoffmann, C.A. Hurni, S. Schartner, M. Austerer, E. Mujagić, M. Nobile, A. Benz, W. Schrenk, A.M. Andrews, P. Klang, G. Strasser, Coherence in Y-coupled quantum cascade lasers, Appl. Phys. Lett. 91 (2007) 161106.
[82] L.K. Hoffmann, M. Klinkmüller, E. Mujagić, M.P. Semtsiv, W. Schrenk, W.T. Masselink, G. Strasser, Tree array quantum cascade laser, Opt. Express 17 (2) (2009) 649–657.
[83] A. Lyakh, R. Maulini, A. Tsekoun, R. Go, C.K.N. Patel, Continuous wave operation of buried heterostructure 4.6 μm quantum cascade laser Y-junctions and tree arrays, Opt. Express 22 (1) (2014) 1203–1208.
[84] W. Zhou, S. Slivken, M. Razeghi, Phase-locked, high power, mid-infrared quantum cascade laser arrays, Appl. Phys. Lett. 112 (18) (2018), 181106.
[85] G. Bloom, C. Larat, E. Lalier, G. Lehoucq, S. Bansropun, M.-S.L. Lee-Bouhours, B. Loiseaux, M. Carras, X. Marcadet, G. Lucas-Leclin, P. Georges, Passive coherent beam combining of quantum-cascade lasers with a Dammann grating, Opt. Lett. 36 (19) (2011) 3810–3812.
[86] V. Daneu, A. Sanchez, T.Y. Fan, H.K. Cho, G.W. Turner, C.C. Cook, Spectral beam combining of a broad-stripe diode laser array in an external cavity, Opt. Lett. 25 (2000) 405–407.
[87] B. Chann, R.K. Huang, L.J. Missagia, C.T. Harris, Z.L. Liau, A.K. Goyal, J.P. Donnelly, T.Y. Fan, A. Sanchez-Rubio, G.W. Turner, Near-diffraction-limited diode laser arrays by wavelength beam combining, Opt. Lett. 30 (16) (2005) 2104.
[88] T.Y. Fan, A. Sanchez, V. Daneu, R.L. Aggarval, S.C. Buchter, A. Goyal, Ch.C. Cook, Laser beam combining for power and brightness scaling, Aerospace Conf. Proc. IEEE 3 (2000) 49–54.
[89] A. Sanchez-Rubio, T.Y. Fan, S.J. Augst, A.K. Goyal, K.J. Creedon, J.T. Gopinath, V. Daneu, B. Chann, R. Huang, Wavelength beam combining for power and brightness scaling of laser systems, Lincoln Lab. Journal 20 (2) (2014) 52–65.
[90] A.K. Goyal, M. Spencer, O. Shatrovoy, B.G. Lee, L. Diehl, Ch. Pfluegl, A. Sanchez, F. Capasso, Dispersion-compensated wavelength beam combining of quantum-cascade-laser arrays, Opt. Express 19 (27) (2011) 26725–26731.
[91] S. Hugger, R. Aidam, W. Bronner, F. Fuchs, R. Lösch, Q. Yang, J. Wagner, E. Romasew, M. Raab, H.D. Tholl, B. Höfer, A.L. Matthes, Power scaling of quantum cascade lasers via multiemiter beam combining, Opt. Eng. 49 (11) (2010), 111111-(1-6).